Environmental Earth Sciences (2023) 82:514
https://doi.org/10.1007/s12665-023-11200-x

ORIGINAL ARTICLE

A catchment scale GPR application potential zonation: case study from SW China

Qiangshan Gao[1,2] · Yawar Hussain[3] · Le Cao[4] · Dandan Cheng[5]

Received: 20 October 2022 / Accepted: 15 September 2023

Abstract
The epikarst together with its soil stocks (subcutaneous structure) are crucial to the fact that they may contribute to the canopy growth and can significantly influence the ecological restoration and organic carbon sequestration. Geophysical techniques especially, the ground penetrating radar (GPR) are advantageous for such investigations. However, the complicated karst environment due to numerous influencing factors (i.e., the forest, epikarst slope, peak-cluster depression, soil humidity, high voltage power lines) can significantly influence the exploration with GPR. In the past, such applications were limited to local scales without considering the aforementioned factors together. Hence, the present study analyses the influences of these factors on the performance and reliability of GPR results considering the central Guizhou plateau of south-west China as a case study. These site-specific findings are summarized into a GPR application potential zonation map at the catchment scale. The zones were rated as low, moderate and high potential degree regions, each reflecting results reliability which can be considered as a cost-effective feasibility reference for the future GPR applications in complex karst terrain characterization, as well as the areas having similar karstic conditions.

Keywords Epikarst slope · Peak-cluster depression · Subcutaneous structure · GPR attribute

Introduction

The epikarst resulted from the dissolution of carbonate rock, is distributed at the intersections of the Earth's lithosphere, hydrosphere, biosphere and atmosphere, which plays a vital role in regulating the natural habitat, supporting the economy and providing ecological services as vegetation growth and organic carbon sequestration at local scale (Yang and Zhang 2014). In this regard, the karst catchment of south-west (SW) China is one of the largest karst concentrated areas in the world, and is special for its high landscape heterogeneity, connection between surface morphology and underground environments (fauna and speleothems) through dualistic hydrological system, and high vegetative endemism (Zhang et al. 2017).

A variety of research techniques and methods have been introduced to study many aspects of karst environment. Among them, the ground penetrating radar (GPR) is prominent, especially in the karst subcutaneous structure investigations such as depth of epikarst and geometry of soil stocks (Al-fares et al. 2002; Zhang et al. 2011; Li et al. 2015; Han et al. 2016; Gizzi and Leucci 2018; Gao et al. 2020). Previous studies mainly focus on the interpretation of the subsurface targets, such as analyzing the corresponding signal responses of epikarst and surface soil in some typical transections and sites. However, the karst environment is complicated and there are considerable geomorphological, geological, climatological and urban factors that can affect the exploration results.

✉ Qiangshan Gao
gaoqiangshan@nssc.ac.cn

1 State Key Laboratory of Space Weather, National Space Science Center, Chinese Academy of Sciences, Beijing 100190, China

2 State Key Laboratory of Environment Geochemistry, Institute of Geochemistry, Chinese Academy of Sciences, Guiyang 550081, China

3 Earth Science Department, Research Centre for Geological Risks-CERI, University of Rome "Sapienza", 00185 Rome, Italy

4 College of Biology and Environmental Engineering, Guiyang University, Guiyang 550005, China

5 China Research Institute of Radio Wave Propagation, Qingdao 266103, China

Published online: 05 October 2023

Among the geomorphological factors, the tree trucks and roots are the significant. However, in the literature, these factors were considered as unnecessary in SW China because of the rocky desertification which prevailed in the past, most areas were considered as the non-growing forest. However, with the growing biomass in the recent years, a major change in the geomorphology has been observed increasing the karst value (Brandt et al. 2018; Tong et al. 2018) and also making it a complicated environment for GPR applications. Many experts successfully studied tree roots architecture by GPR signal response (Tardío et al. 2016; Zajícová and Chuman 2019; Alani and Lantini 2020). However, the signals reflected from the roots can affect interpretation of the subsurface structures. The influential geological factors include the uneven tomography (epikarst slope, peak-cluster depression (PCD) and peak-cluster valley) and the indented soil–rock interface which can make the propagation paths of radar waves intricated and cause tilting in the GPR image and subsurface depression identification become challenging (Gao et al. 2022). The climate of SW China is tropical with rainy and dry seasons with a variable soil humidity throughout the year. The high value of humidity directly related with the electrical conductivity which decreases the GPR depth of penetration (Campbell 1990). The traditional interpretation method is delineating maximum depth of dense strong amplitude area in GPR image as epikarst depth (Al-fares et al. 2002; Zhang et al. 2011), which ignores weak amplitude reflected by some epikarst clutters. The anthropogenic factors, such as houses, bridges and highway can badly affect the GPR results because of the damages these structures have done to the original soil-rock structures.

The aforementioned factors reported in the literature were studied individually and at local scales. Few studies were reported on catchment scale in USA for soil surveying using GPR calibrated with field observations (e.g., Johnson et al. 1979; Schellentrager et al. 1988). Doolittle et al. (2003, 2007, 2010) developed and later revised GPR soil suitability map using the national soil attribute data, and GPR results obtained with different antennas of frequency ranged between 100 and 200 MHz. This GPR soil suitability map highlights its expected penetrating depth in different areas of USA into six levels ranges from high to low. The map just focused on the influence of soil properties on GPR signal propagation, not considering the influencing factors generated by the topography and vegetation.

The condition of GPR exploration in karst area is different with in non-karst areas. Just considering the GPR soil penetration is not appropriate to study the complicated karst environment. More efforts to evaluate the GPR application potential to karst areas with more known influencing factors synthetically is necessary. As a case, the present study was dedicated to map the GPR application potential by considering the result from five studied sites distributed in the Houzhai catchment, a typical karst catchment in SW China. The catchment is a focus of many investigations because of its high ecological values. The present study is divided to two stages, (1) in the first stage, the effects of different factors on GPR results are assessment and (2) next, the present study proposes a ranking criterion based on field observations, digital evolution model (DEM), and vegetation map to rank the GPR application potential. Finally, the contribution of the factors to the potential degree evaluation for the catchment has been discussed and some possible combinations of geophysical methods are recommended for solving problems that are difficult to assess with GPR data alone. Apart from the site specification in any GPR manuals, the study can be seen as a cost-effective feasibility reference for layman before a karst project starting.

Study area

The Houzhai catchment is located in the south of Puding county, Guizhou province, and belongs to the heartland of karst area of SW China. This area has western ocean pacific subtropical monsoon humid climate, May to October is classified as the rainy season, accounting for 83–88% of the total annual precipitation (Cheng et al. 2019). The red clay (terra rossa) is the main soil type found in the area which is formed as a result of carbonate dissolution under local climatic conditions (Zhou et al. 2012). The karst landforms are well developed leading to the formation of typical karst surface and subsurface hydrogeological structure in the catchment.

The Houzhai catchment is located in the watersheds of the Pearl and Yangtze River systems. The catchment terrain presents a southeast-northwest elevation gradient. Both surface and subsurface rivers originate in the east of the catchment, flow to the northwest, and eventually merge into the Sancha River in north of Puding country, eventually flowing into the Yangtze River. From the upstream to the downstream, a change in geomorphic features occur as peak-cluster depression, peak cluster valley, peak forest basin and peak forest plain (Fig. 1). The surface and subsurface rivers have the closure feature, no other exogenous river passing through, and has independent small karst environment (Zhang et al. 2018). Therefore, studying the catchment can give the significant implication of karst process, which appealed numerous scholars to implement research (e.g., Li et al. 2010; Barna et al. 2020). For example, analysis of the material composition of soil samples from the upstream and downstream in the catchment allows an assessment of the main types of soil that are mostly eroded away from karst area (Cheng et al. 2020).

In the initial stage, a detailed investigation based on the literature and using Google imagery has been carried for the identification of potential study sites where GPR influencing

Fig. 1 The red dots on the DEM of the Houzhai catchment area marked the GPR acquisition sites along with important hydrological features of interests. The insert shows the SW China map

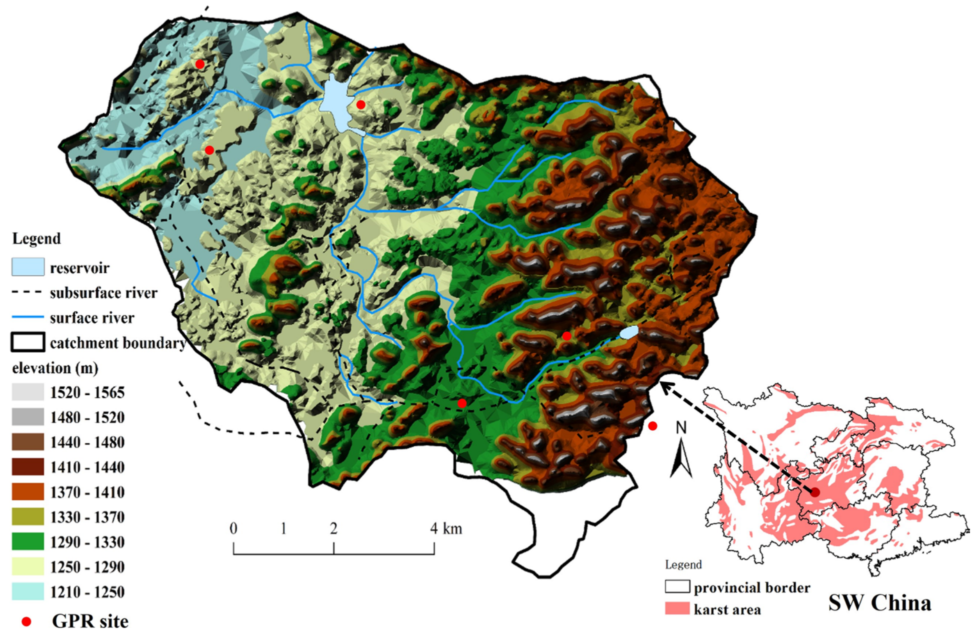

indicators are well exposed and are easily reachable. Based on these reconnaissances, the GPR experiments have been executed at the numerous different sites. Through comparison, the results of five sites (karst slope, PCD, forest site-1, forest site-2, paddy land and grass land under HVPL) reflected the general GPR features under different influencing factors. The geographic locations of the five sites studies are marked on the DEM are shown in Fig. 1. The details about the acquisition and setting for instrument testing are provided in Table 1.

Methodology

The ReflexW software was used for the processing which included the direct wave removal, zero drift elimination, amplitude gain, horizontal signal interference removal, bandpass filtering, data smoothing. The F-K filtering method is applied to transform the GPR data into the frequency wave-number domain for suppressing or eliminating the coherent interference signals (Jol 2009). The processed details using ReflexW software can be found elsewhere (Gao et al. 2022). After that the GPR attribute analysis (i.e., average energy, amplitude and coherence) is carried out as the last data processing step, each of which can highlight one aspect/feature of the traditional GPR data and were demonstrated the unique value in the archaeological prospection (Zhao et al. 2013) and karst studies (Reis et al. 2014). The average energy and coherence attributes are extracted to aid in interpretation of the soil–rock interface through the analysis of important features in the signals. The average energy attribute was applied to reflect the position of soil and rock by showing energy contrast of signals (Gao et al. 2020). The coherence attribute quantitatively describes the waveform similarity of the adjacent traces (Bahorich and Farmer 1995). This attribute highlights the waveform information by excluding the energy/amplitude feature of signals. The epikarst depth interpreted by coherence attribute is generally

Table 1 GPR acquisition parameters with the details of instrument used at each site

Site	Coordinates	Antenna	Sampling mode	Trace/time interval	Sampling rate (MHz)
Karst slope	26°13′ 16.6″ N, 105°45′ 23.2″ E	500 MHz shielded	Wheel	0.019 m	7695.4
Peak cluster depression	26°14′ 01.9″ N, 105°46′ 10.3″ E	500 MHz shielded	Wheel	0.019 m	7819.5
		50 MHz RTA unshielded	Time	0.5 s	623.9
Forest site-1	26°16′ 25.1″ N, 105°42′ 31.0″ E	50 MHz RTA unshielded	Time	0.5 s	599.9
Forest site-2	26°16′ 27.5″ N, 105°43′ 47.5″ E	50 MHz RTA unshielded	Time	0.5 s	599.9
Paddy land	26°13′ 21.5″ N, 105°47′ 40.1″ E	50 MHz RTA unshielded	Time	0.5 s	599.9
Grass land under power lines	26°15′ 09.5″ N, 105°42′ 6.0″ E	50 MHz RTA unshielded	Time	0.5 s	599.9

deeper than that of the traditional method inferred from work of Gao et al. (2020) and Hussain et al. (2023). The values are presented over a range from 0 to 1. Higher values indicate a strong similarity between the traces, and vice versa.

We applied the conventional/traditional and attribute data which are commonly used in the GPR interpretation to evaluate the exploration results of the following sites. The basis of forming the quantitative or qualitative experiment is the extent that GPR data can acquire the subsurface information. Note that the data are processed by the conventional methods of GPR manuals. The region where the data interpreting subsurface without worrying about significant interferences and all acquired information could be interpret subsurface is seen as low difficulty and high application potential. We consider the moderate difficulty and application potential region where just partial data information could be used to interpret subsurface and other possible valid information mixing with interferences, difficult to filter out dividually. The site where the data information being contaminated completely by interferences difficult to eliminate is considered as high difficulty and low application potential.

Results

Karst slope

We primarily studied the karst slope, whose important feature is the epikarst that has many fissures filled with soil. The fissure density of epikarst decreases with depth (Al-fares et al. 2002). A typical epikarst example including indented soil–rock interface and undulating bottom of the karst slope profile is shown in Fig. 2. This profile has been also investigated by geophysical techniques by Tao et al. (2022), which was further enhanced by including the GPR attributes analysis for the delineation of rock and soil media exposed to the surface (Gao et al. 2020).

It can be seen in Fig. 3a that the lateral position of soil exposed to surface is generally corresponding to low energy value while rock presence reflects high energy value. But from the vertical perspective, the confirmation of soil depth and indented soil–rock interface delineation is challenging and depending on the energy contrast of GPR data (Fig. 3a). Additionally, the lower boundary of epikarst can be interpreted well by the general interface of valid and invalid signals reflected by the coherence attribute. The reflection signals of the layer C under the epikarst exclude the possibility of GPR pulse signal attenuating to zero when propagating to the epikarst lower boundary (Fig. 3b).

In case of high water content, the reflection signals of layer C cannot be seen clearly making the interpretation of epikarst lower boundary obscure. Following two possible situations can be plausible. First, the pulse signal energy attenuates to zero or the level of random noise before transmitting to the epikarst bottom, thus the interface of valid and invalid signal regions just reflects the maximum penetrating depth of radar wave. Another situation could be the triggered signal attenuates to zero or the level of random noise as propagating between epikarst bottom and the lower layer C. Therefore, the incomplete subsurface information about karst slope can be retrieved from GPR application.

Peak-cluster depression

As one common geomorphic unit in the karst area, PCD consists of peak cluster hills with steep slope and uneven relative heights and the depression with different sizes and different shapes. The soil–rock interface under the

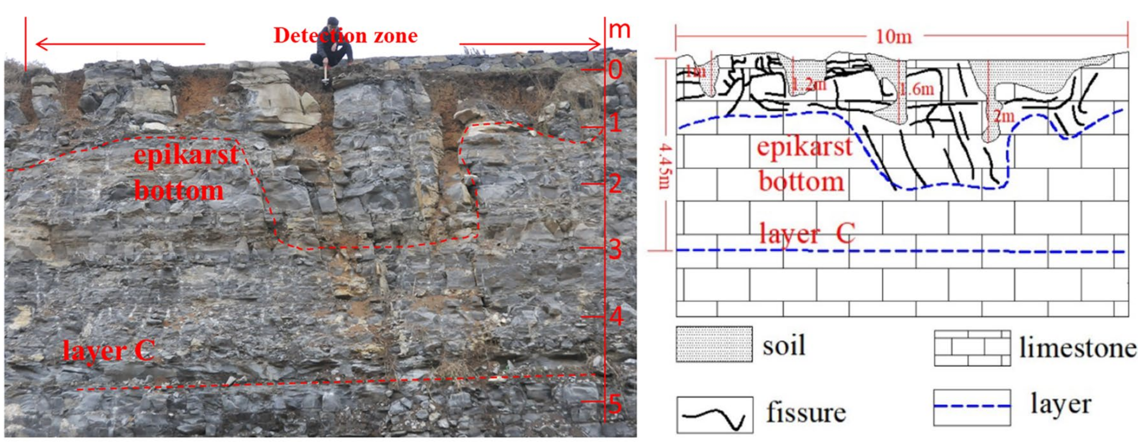

(a) (b)

Fig. 2 **a** The photograph of a typical karst slope found in the region. The upper red dotted curve line is lower boundary of epikarst and the lower dotted line is bedding layer. **b** GPR driven cross-section showing epikarst indented soil–rock interfaces (revised from Gao et al. 2020)

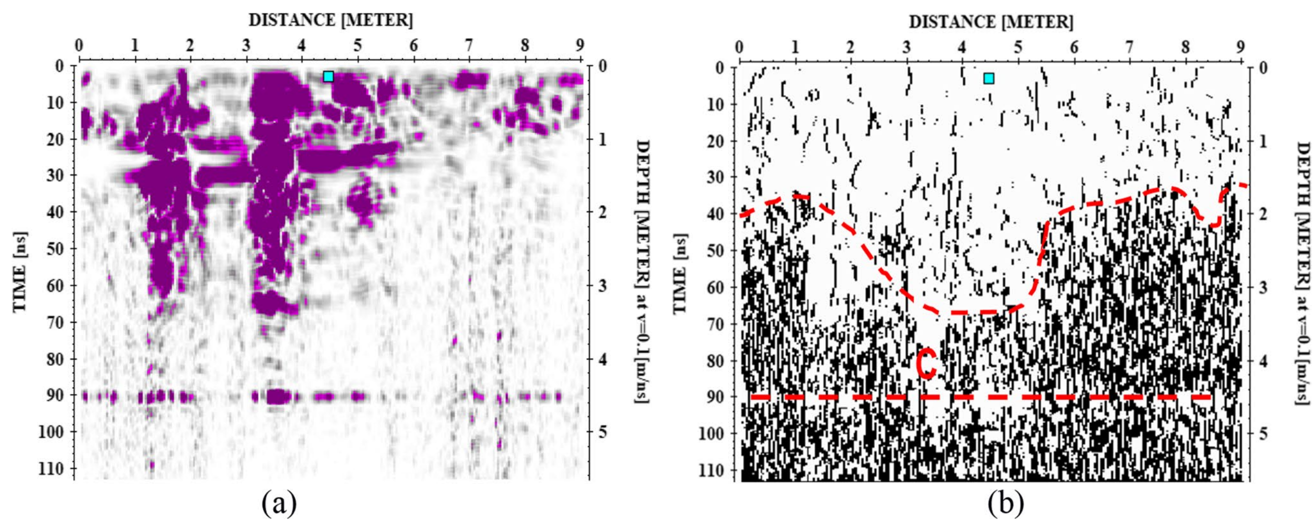

Fig. 3 **a** The average energy attribute and **b** coherence attribute acquired on a karst slope adopted after Gao et al. (2020). The bright shades of purple are high energy value and dull white and grey is low value. The cyan block mark corresponds to position of the hammer in Fig. 2a and fissure with soil. The upper red dotted curve line in the right panel draws the epikarst bottom interface interpreted by GPR attribute

depression can not be completely vertical or horizontal because of the great topography variations in karst area as concluded from numerous previous field observations. On the other hand, Chen et al (2006) found that the depression soil moisture content changed greatly in the depth range of 0–30 cm at a PCD from Guangxi karst area. In another study, the GPR applicability was tested by forward modelling and actual data were analyzed in details (Gao et al. 2022).

The GPR forward research about the depression highlighted the effects of surrounding hills, inclined soil–rock interface and soil conductivity (Fig. 4). Through multiple numerical modelling with different conductivity parameters setup, the forward results demonstrated that the tilt signals/events in GPR image contained the reflection (or linear back-scattering) waves both from the hills and the underground inclined interface with equivalent amplitude over an appropriate soil conductivity range.

The field observations of GPR data constitute of acquisition with unshielded 50 MHz RTA on the Zhongba depression situated in the Houzhai catchment (Fig. 5). As a result, several tilt signals are emerged on the radar image (Fig. 6), possibly related with the typical karst hills and surrounded by ancient vegetation cover (see Yan et al. 2012). However, the real field conditions of the PCD are much more complex than that of what is depicted in the forward model. The auger verification demonstrated that the retained horizontal signals can provide information of the internal soil layers in depression while information about the inclined interface information is lost. Thus, the accurate source of the tilt signals is difficult to confirm. Hence, partial or incomplete information about

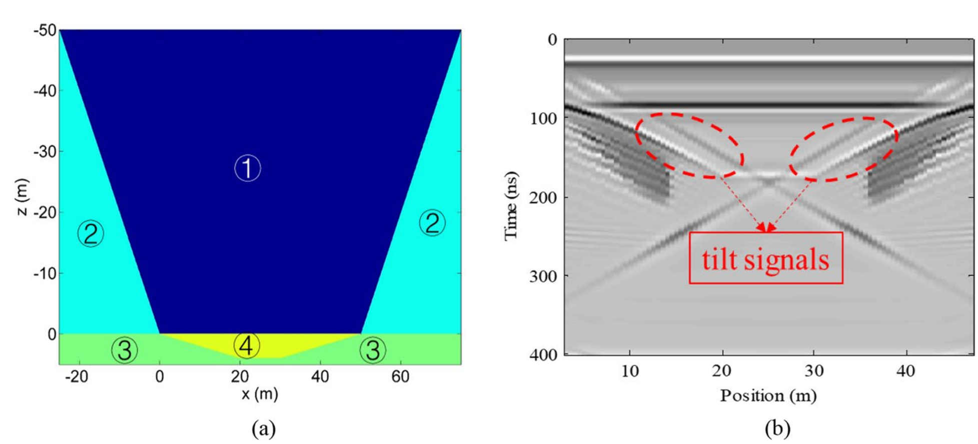

Fig. 4 **a** the forward model of PCD and **b** its forward result by FDTD. The annotations ① represent the air, ② the hill, ③ the bedrock, and ④ the soil of the depression (adopted from Gao et al. 2022)

Fig. 5 Photographs of **a** Zhongba depression, red arrow marks the GPR survey line and direction and **b** GPR acquisition revised according to Gao et al (2020)

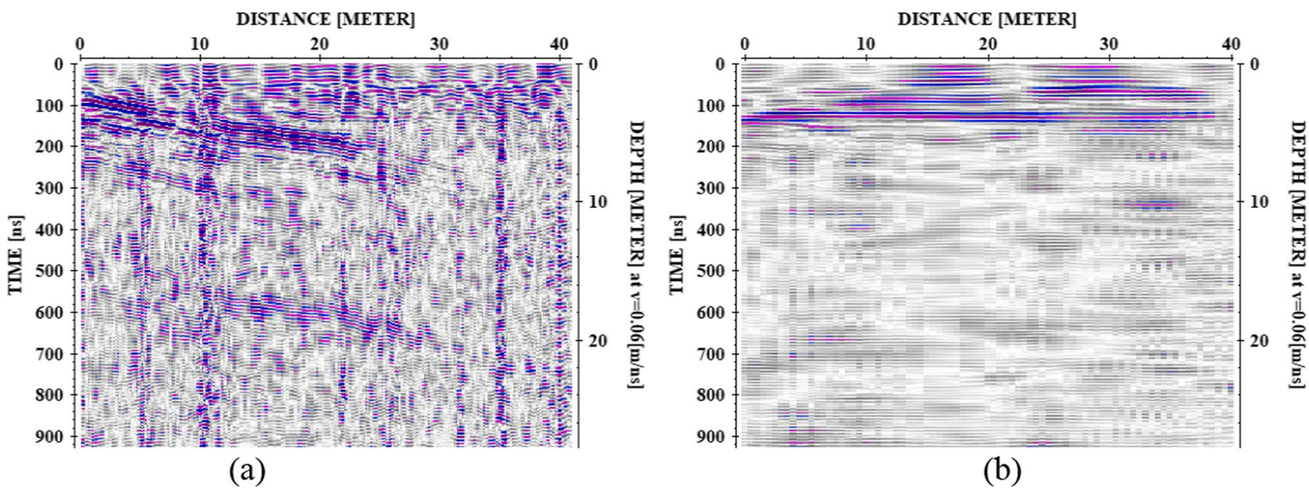

Fig. 6 **a** Conventional GPR images of the Zhongba depression and **b** processed applying F-K filtering revised from Gao et al. (2022). Right tilt signals can be seen clearly while the left tilt signals have some difficulty to observe in the **a**

depression soil can be acquired using low frequency antenna possibly because of the interference coming from the surrounding hills. The details about GPR processing workflow and associated challenges can be accessed at Gao et al. (2020, 2022).

Comparative to the previous studies, for the present work, data was acquired with 500 MHz shielded antenna along with the same profile as adopted in previous studied (Fig. 5). The GPR image obtained with high-frequency antenna usage is shown in Fig. 7. Though the measured data is not affected by the reflection from hills, the radar wave of high-frequency could not penetrate into the bottom of depression soil. The valid signals just occupy the 20 ns, correspond to less than 1 m of soil depth. The high-frequency antenna is not suitable for interpreting the depression soil depth.

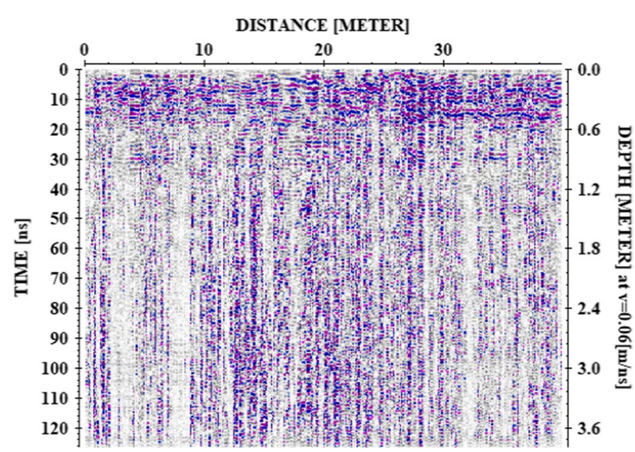

Fig. 7 GPR data image acquired by the shielded 500 MHz antenna

Tree trunks and roots

The major landuse found in the Houzhai catchment is the forest, an indicator of large thick soil stocks in the karst settings. Two such forest sites (referred to as forest site-1 and forest site-2) were chosen for the GPR acquisition with 50 MHz RTA antenna, details are provided in Table 1. The forest site-2 lies next to a large water reservoir, where the surface rivers converge, in the catchment (Fig. 8). Most of the tree trunk diameter is more than 10 cm which is resolvable with the GPR usage. The large heights of the trees indicate the existing of well-developed root systems which are beneficial to reflect radar wave.

Contrasting to the GPR images of these two forest sites (Fig. 9), the valid signals of the site-1 can last more than 300 ns, while that of the site-2 last less than 200 ns. This phenomenon also indicates that the site 2 has higher soil conductivity than the site 1, which conforms to usual respected results. On the other hand, lots of tilt signals can be seen in the images. According to the analogy derivation of the forward study result of the peak-cluster depression, we speculate that the tilt signals include the waves reflected by the tree trunks, the subsurface inclined interface and the waves reflected by tree roots. The complicated tree roots system makes the interpretation of tree land soil structure and epikarst depth more difficult. Therefore, we deem that the accurate information of soil distribution in karst forest land is highly difficult to obtain by GPR due to the mix of tree trunks and roots reflection signals. The epikarst survey over the woodland soil layer is challenged by the presence of more prominent influencing factors as deeper soil with high moisture contents.

The high-frequency antenna is more convenient in detecting the roots system (Alani and Lantini 2020). Though the reflection signals of the trunks have been shielded, the complicated roots system can still make the soil and epikarst interpretation difficult with the data acquired using 500 MHz antenna.

Rainfall and soil moisture

The effects of soil moisture in delineation its depth was investigated using a paddy land acquisition with 50 MHz RTA antenna (Fig. 10). The survey was planned immediately

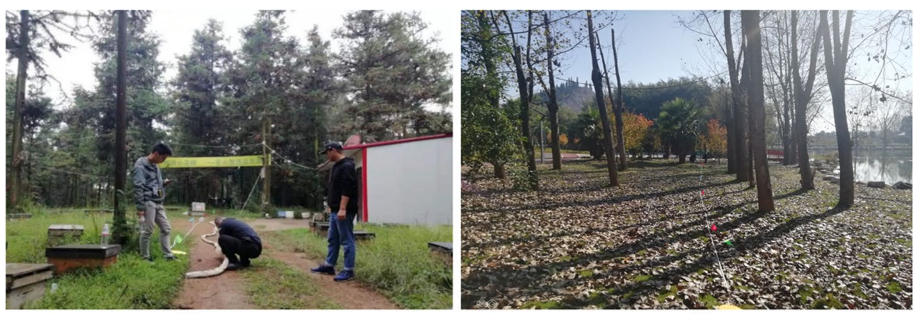

(a) (b)

Fig. 8 **a** Site-1 and **b** site-2 of forest land. The site-2 is close to a water reservoir

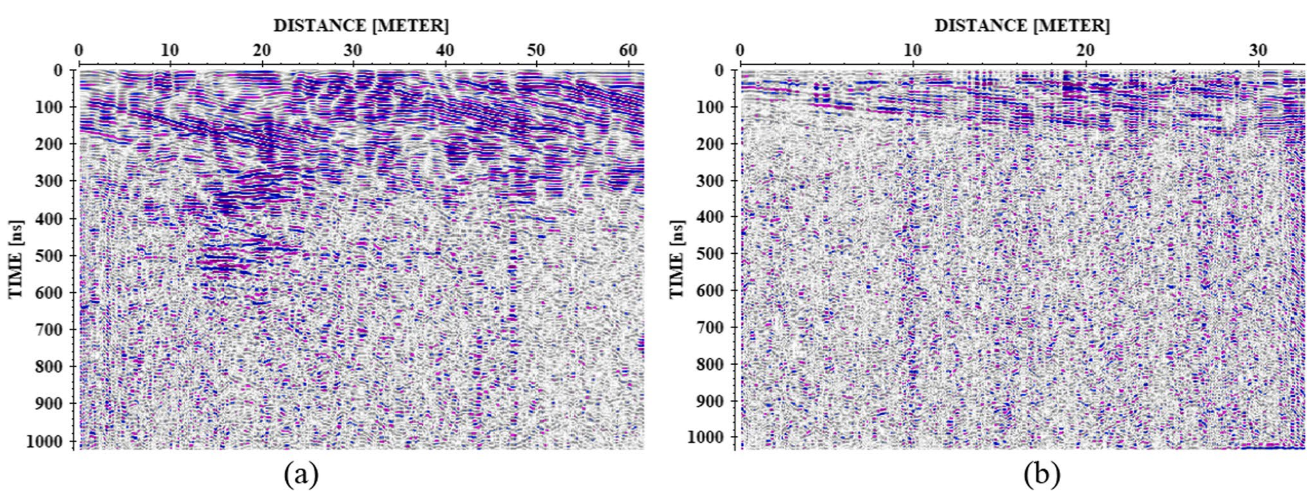

Fig. 9 GPR images of the **a** site-1 and **b** site-2. Some tilt signals coming from the reflection of tree trunks and roots may mix with the other tilt signals from the subsurface inclined interfaces

Fig. 10 Photograph of investigated paddy land. The surface soil moisture content is ~ 31.8% by measurements in situ

after the completion of rice harvest which provided a condition where the water had already seeped into the ground, which increased the soil moisture content along the depth. The surface soil moisture content was measured as ~ 31.8%, which can almost represent the maximum of soil moisture in karst area (Yang et al. 2019).

Analyzing the measured GPR data and its coherence attribute (Fig. 11), we found the majority of signals have weak amplitude and low similarity, which fit the features of random noise interference (Jol 2009). This suggests that radar waves almost cannot penetrate soil layer with more than 30% moisture content.

High-voltage power lines (HVPL)

Three high-voltage power lines pass through the studied site in the Houzhai catchment. These lines generate a strong electromagnetic field. The low-frequency GPR data are affected by these lines within the 100 m range by setting GPR survey orthogonal to power lines (Cheng et al. 2010). For the impact assessment of these lines on GPR with unshielded antenna is acquired in parallel to the lines under the lines in the grass land (Fig. 12). Results showed a highly contaminated data with similar pattern strong signal interference (Fig. 13). Processing with F-K filtering suppress the strong amplitude signals but the interference with high similarity pattern is still present on the coherence attribute image (Fig. 14). Therefore, the application potential evaluation of GPR survey must consider the influence of HVPL proximities.

Fig. 12 Photograph shows GPR acquisition on grass land under high voltage lines

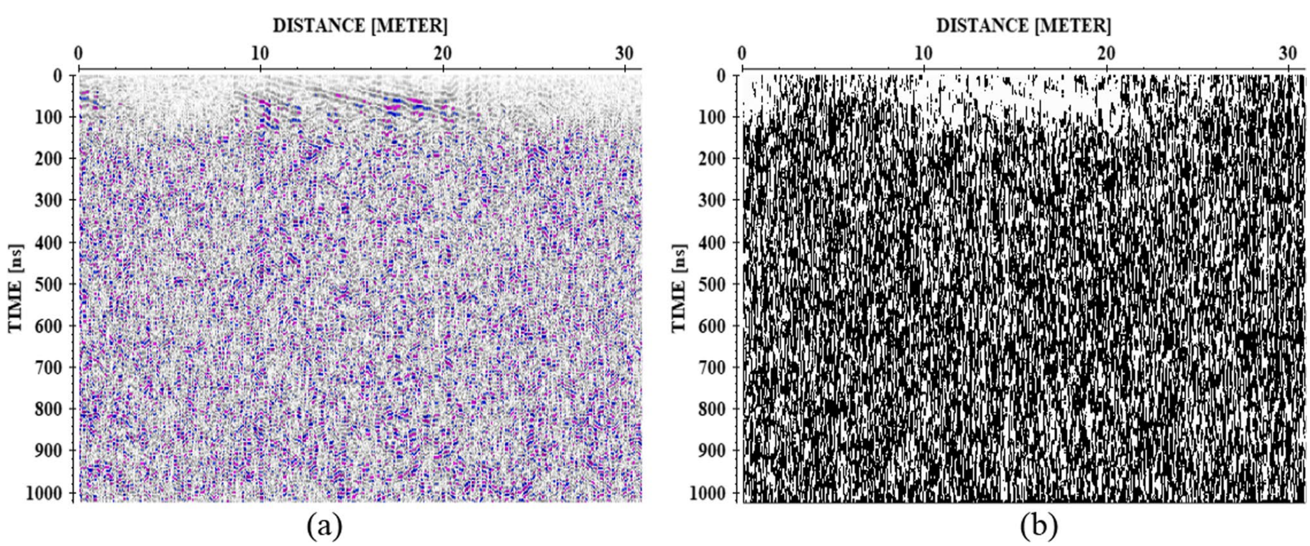

Fig. 11 GPR data of the **a** paddy land and **b** its coherence attribute, the black color is low value and the white is high in the coherence image

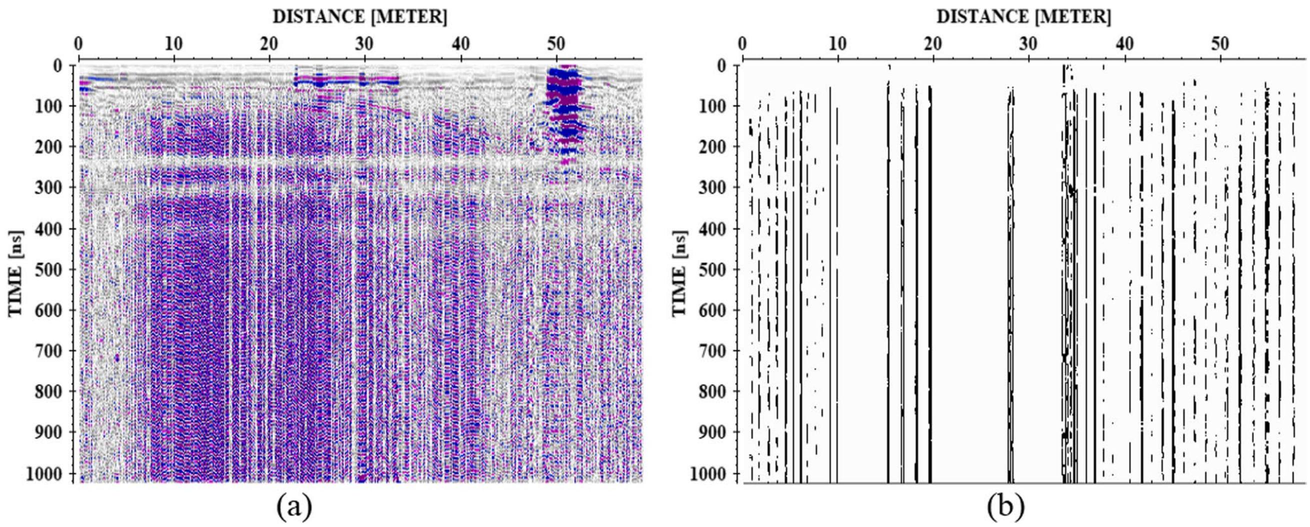

Fig. 13 **a** Conventional GPR image and **b** its coherence attribute

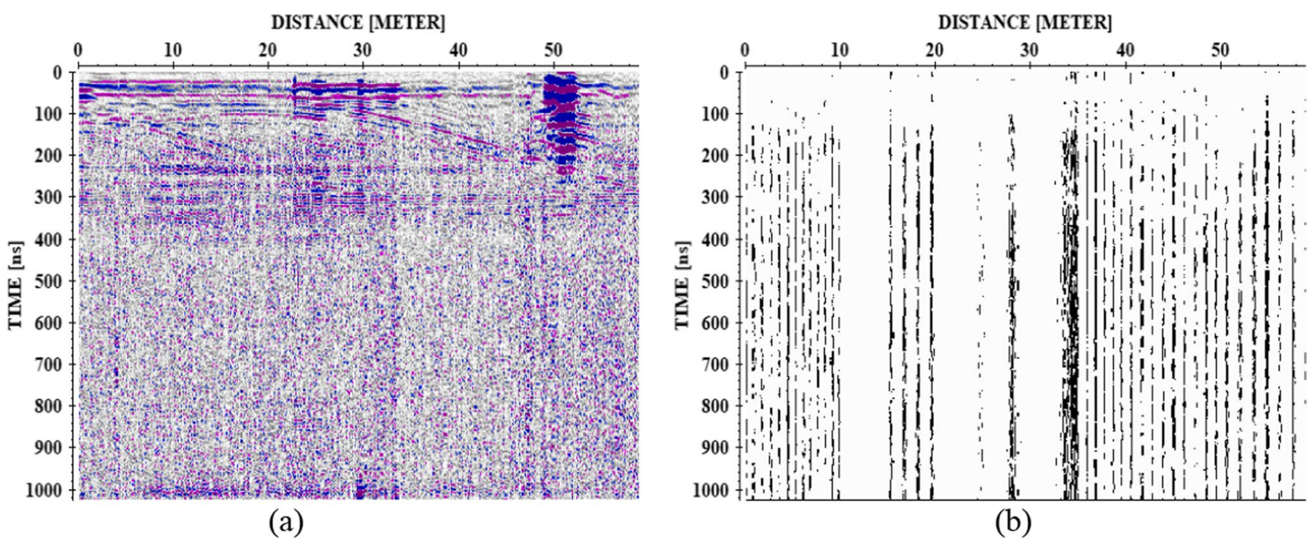

Fig. 14 Results of data **a** near HVPL proximity with **b** F-K filtering and its coherence attribute image

Application potential evaluation

The catchment scale application potential evaluation of GPR data acquired using 50 MHz RTA and 500 MHz shielded antenna in detecting karst surface structure in the Houzhai catchment is carried out. During the acquisition, the catchment was divided into three regions as low, moderate and high potentials, based on field observations, the topography, and vegetation cover map (see the Appendix). Different potential degrees reflect the reliability of GPR data interpretation for soil distribution and epikarst depth by considering surface and subsurface influencing factors. Table 2 summarizes the findings of the present study as well as inferred from literature review.

Over the regions of low applicability potential (e.g., forest lands and sites under HVPL) the GPR data show multi-source interferences leading to difficulties in interpretation of the soil and epikarst. Most of the forest lands are mainly found in the peak-cluster depression and peak-cluster valley of the catchment. The influencing factors here include tree trunks, roots system, HVPL, soil depth and moisture contents. The diameter of tree trunk is usually more than 10 cm, reaching the resolution of the 50 MHz and 500 MHz antennas. The reflection from trunks and roots are mixed

Table 2 The potential degree evaluation of GPR applied to the Houzhai catchment

Potential degree	Corresponding geomorphic region and land use	Influencing factors	Effect of interpreting soil distribution for 50 MHz RTA and 500 MHz shielded antenna	Effect of interpreting epikarst depth for 50 MHz RTA and 500 MHz shielded antenna
low	Forest land, high voltage line within 100 m range	Tree trunk, tree root, high-voltage lines, moisture content, soil thickness	Bad effect for two kinds antennas, great multiple solutions, High difficulty to interpret due to signals overlap of trunk, root and inclined interface reflection Poor methods to filter interference	Bad effect for two kinds antennas, Great multiple solutions, High difficulty to interpret with further considering the soil thickness and moisture content, High difficulty to confirm the epikarst depth
Moderate	Karst slope, bottom of peak cluster depression, bottom of peak cluster valley	Moisture content, Soil layer thickness, Hills reflection	Interpret the soil structure in karst slope is moderate difficulty for 500 MHz but high difficulty for 50 MHz Moderate difficulty in the depression and valley for 50 MHz RTA due to the tilt signals overlap, 500 MHz antenna is not suitable in the depression and valley due to the soil thickness and moisture content	Shallow karst cave or pipelines under karst slope can be possibly detected by 50 MHz, more difficulty for 500 MHz; Interpretation difficulty of epikarst depth increases from top to foot of karst slope for both antennas Reflection signals of epikarst inclined interface under valley and depression can overlap with the hill reflection signals for 50 MHz if soil layer is not too sick
High	Basin, plain, agricultural land use	Soil layer thickness, moisture content	Soil layer depth and soil–rock interface can be quantitatively interpreted for 50 MHz RTA. The accuracy can be verified by auger High difficulty for 500 MHz to penetrate soil bottom	High difficulty to interpret epikarst under the soil layer for two kinds antennas Epikarst information may not be acquired when soil thickness is close to 4 m for 50 MHz RTA, shallower for 500 MHz

with those from subsurface media, making the GPR results obscure and separation of real sources of either horizontal or tilt signals challenging. Tall and dense growing trees imply a large amount of soil with a relatively large thickness. The limit of depth of soil penetration for high frequency antenna is questionable. The electromagnetic field generated by the HVPL resulted in the non-eliminable interference contamination in the GPR data.

The moderate applicability potential regions are the areas where partial information of the target is retrieved from GPR while the rest is lost by the attenuation and/or overlapping of signals. The peak-cluster depression and peak-cluster valley bottoms and slope without forests can be classified into this category. The influencing factors include reflections from hills, soil thickness and moisture content.

The effects of karst slope on GPR results vary with the frequency of antennas and distribution of soil which becomes deeper and heterogeneous from upslope to downslope. The epikarst depth also increases gradually in downslope direction. The shallow and discontinuous surface soil is suitable for low-frequency antenna to detect caves (Čeru et al. 2018; Hussain et al. 2020). Generally, shallow caves or pipelines are deeper than epikarst lower boundary and could be detected in favorable conditions such as thinner and dry soil. The reflection from caves or pipelines can also account for GPR signals penetration till epikarst bottom. But it is difficulty for 50 MHz data to interpret the upslope fissure soil distribution due to low resolution and little soil distribution. As for the 500 MHz antenna, the interpretation of slope epikarst bottom require lower moisture in theory. The GPR coherence attribute is beneficial in interpreting the valid and invalid signals interface, which may correspond to the epikarst bottom (Gao et al. 2020). However, the level of difficulty in interpreting epikarst bottom depth increases from upslope to downslope due to the increase of soil thickness and moisture content.

The use of low-frequency antenna is recommended for the exploration of soil layer bottoms in peak-cluster depression and valley. In terms of unshielded 50 MHz RTA, the signals reflected by hills overlap with the signals reflected from the subsurface inclined interface due to the depression and valley close to hills, making difficult to accurately confirm the exact source of tilt signals. The tilt signals can be eliminated by F-K filtering, and the retained signals can reflect the depth of soil lateral layers and soil–rock interface in the depression and valley by the average amplitude and coherence attributes (Gao et al. 2022). Unfortunately, the information of the inclined interface is lost. The surface of depression and valley is usually entirely covered with the soil layer which is deeper than that of soil found on slope. Additionally, the bottom of karst peak-cluster depression and valley is a sink for the rainfall and runoff from the adjoining areas. Therefore, these are generally the regions of high soil moisture contents than that of slope soil. It is challenging to detect the epikarst depth under the depression and valley using low-frequency antenna.

Summarizing the above GPR interpreting effects of high and moderate regions with high and low center frequency antennas, we summed up above results and drawn the key

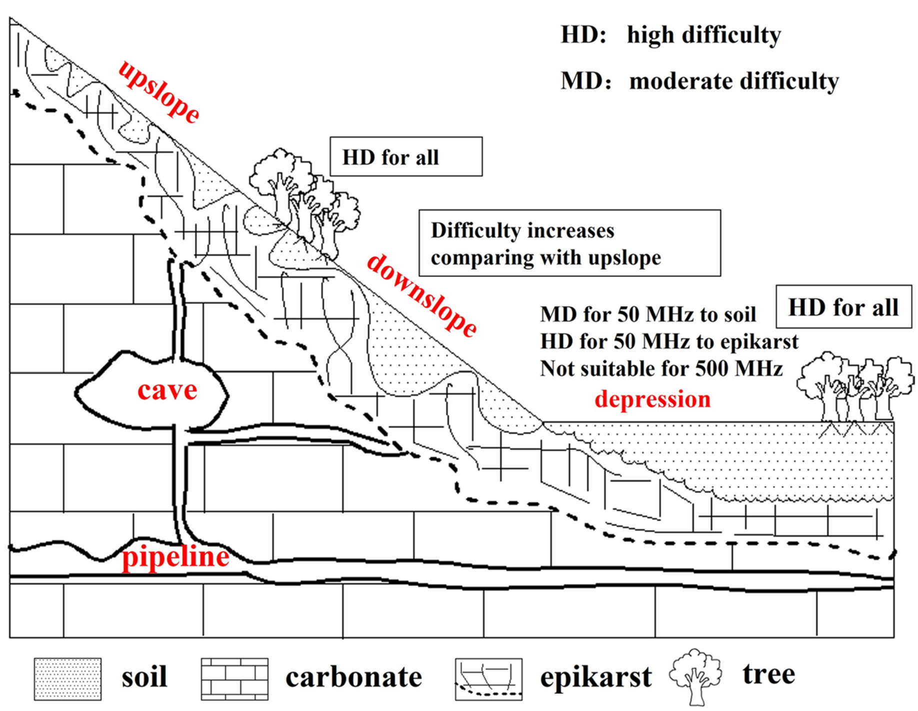

Fig. 15 The conceptual diagram explaining different aspects of GPR potential evaluation in peak-cluster depression study

information into one simple conceptual diagram shown in Fig. 15.

High application potential is the region where GPR information is solely obtained from the subsurface structures without having any influence from the external factors as explained above. This region corresponds to the basin and plain of the catchment, excluding the sites covered by forest. Results of GPR data acquired from this region have high reliability in the soil and epikarst delineation. The soil distribution can be interpreted by analyzing the average amplitude and coherence attributes and results accuracy can be verified by drilling. However, GPR acquiring the depth information of epikarst under relatively thick soil layer is most difficult. The limited thickness of soil layer can be referred to the example of the Zhongba depression. The thickness and water content of soil layer are usually higher than those of slope. The thickness of soil layer in the Zhongba depression is ~ 4 m (Gao et al. 2020). The measured data was acquired in the premise of no rainfall event and hot weather lasting more than a week. The 50 MHz antenna just detected the maximum depth of the soil layer and did not receive the echo signals of the deeper epikarst. Thus, we simply consider the soil thickness close to 4 m is not conducive for low frequency antenna to obtain the structure information of epikarst. As for the 500 MHz antenna with high resolution, its requirement for the soil thickness is much shallower.

The above information is summarized in one rough map about the GPR application potential evaluation in the Houzhai catchment using DEM, the vegetation data and locations of HVPL (Fig. 16).

Considering the seasonal variability of climatic conditions in the Houzhai catchment, the soil moisture content changes from low to high with dry to rainy seasons, receptively. The rainy period is not a good time for GPR survey because of high soil conductivity. We recommended the months of October and November as the best time for GPR acquisition in the catchment. On one hand, this period is at the end of the rainy season and the soil in dry season has relatively low moisture content and conductivity (Yang et al. 2019). On the other hand, the most of the places of the low uncertainty region is the farmland. October and November are the period between the summer crop being harvested and the winter crop not fully planted.

Discussion

The application potential evaluation results showed that GPR technology is beneficial in detection of partial subsurface structures in the karst catchment. The application potential of GPR is a function of the influencing factors. Different factors give different contribution of the zonation. Referring to the ideas of GPR suitability index provided by Doolittle et al. (2003), we tried to assess the contribution of each factor within the indexes or scores according to the field experiences. Table 3 shows the assessment results of the influencing factors. The different index values reflect the influence degree of different factors. We tried to give a rating of the three different application potentials based on the contribution assessment of the influencing factors as shown in Table 4. The sum of the influencing indices existing in one site represents the potential levels of the site.

The key thought of determining the numerical values is to assure the sum of influencing index consistent with GPR

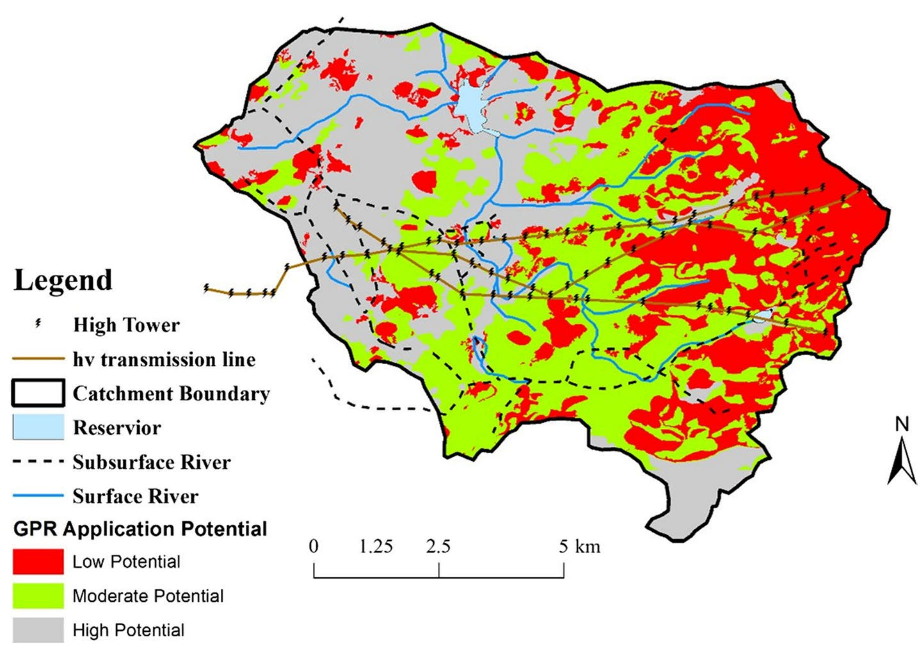

Fig. 16 GPR application potential categorization for the Houzhai catchment

Table 3 the index of each influencing factor

Factors	Influencing index
Tree trunks	2
Tree roots	2
High voltage lines	4
Hills reflection	2
Soil thickness	1
Moisture content (≥ 30%)	4
Moisture content (~ 20%)	1

Table 4 GPR potential ratings based on indices of the influencing factors

GPR categorization index	Potential
≤ 2	High
> 2 to ≤ 4	Moderate
> 4	Low

potential ratings. The influencing factors of soil thickness and moisture are almost everywhere in the catchment. The high application potential region usually just influenced by these two factors. The index value of soil thickness and ~ 20% moisture content setting as 1 can assure their sum being 2 and belonging to high potential index. Due to the media reserving ≥ 30% moisture content not suitable for GPR work, its value is determined as 4, making sure that the sum value with soil thickness as 5 (> 4) which belongs to low potential index. The index of hill reflection setting 2 can assure it exceed the high potential index and the sum plus soil and moisture (~ 20%) be 4, belonging to the moderate potential index. The previous results let us know that just the forest can make the application potential to be low, let alone adding more other influencing factors. Thus, setting the scores of both trunks and roots as 2 can make sure the trees index value be 4. The index of forest region is greater than 4 after adding the influence of soil thickness and moisture content, belong to low potential index. The index value of HVPL determined as 4 is based on similar thought of the forest.

The GPR application potential evaluation resulted in answering the value able questions in the catchment. Some karst structural features can be reflected by GPR data. However, some factors limit the position and time of GPR detection. Combining other geophysical methods, such as electromagnetic (EM) induction, electrical resistivity tomography (ERT) and seismic exploration, can increase the GPR application value for karst exploration.

GPR, EM induction and ERT all realize the detection purpose based on the electrical difference of subsurface media. The integrated use of EM induction and GPR can increase the confidence of interpreters in the interpretive results about karst structures (Doolittle and Collins 1998). ERT can give the characterization of soil-rock interface and sinkhole from another perspective comparing with GPR (Carbonel et al. 2014). The combination of GPR and ERT enhances the delineation of the soil–bedrock interface and identification of the fracture network in the karst areas (Tao et al 2022).

Seismic exploration utilizes the elasticity and density difference of subsurface media to identify the underground structure by triggering seismic waves, which consist of P- and S-wave velocities. The P-wave velocity decreases with increasing soil water saturation and its attenuation is more in dry than in wet soils (Carcione et al 2003; Ding et al 2014). The seismic exploration methods are more suitable for the high moisture content conditions and had been successfully applied to monitoring the subsurface water levels depth (Desper et al 2015; Pasquet et al 2016). Because of the different soil moisture content, ERT has higher accuracy detecting soil depth at upslope and seismic method has higher accuracy at downslope (Coulouma et al 2012). The field survey results in European karst regions concluded that the combination of seismic and electromagnetic methods can be considered as powerful tools for mapping complex karstic environments (Šumanovac and Weisser 2001; Valois et al 2011), as also demonstrated in Fuling area of SW China (Guo et al 2021).

Therefore, the integrated use of geophysical methods to the karst catchment can overcome the spatial and time limitations of electromagnetic methods and provide a detailed information on the deeper targets. Figure 17 shows an application potential paradigm of GPR in the karst catchment.

This is a preliminary study where many of the complicated factors are ignored. The design of GPR antennas is one of them. The transmitter and receiver antennas have fixed spacing, which is very convenient for the flat surfaces, such as the surfaces of highway and tunnel. The uneven surfaces of karst are not conducive to the layout of GPR survey line which is not completely designed for karst environment. Only one receiver is designed to acquire echo resulting that too much information has been lost. We recommend the future work should consider the design of GPR for karst surfaces. For example, similar to the seismic data acquisition, design one antenna to transmit signal and several antennas to receive signals, the spacings of antennas should not be fixed and could be setup by users' will. In case where GPR equipment are specially designed for karst, the application potential evaluation results will be probably different.

Summary

In view of the lack of macro-evaluation of GPR applied to karst catchment and facing many influence factors, this paper summarized the detection effects of GPR field

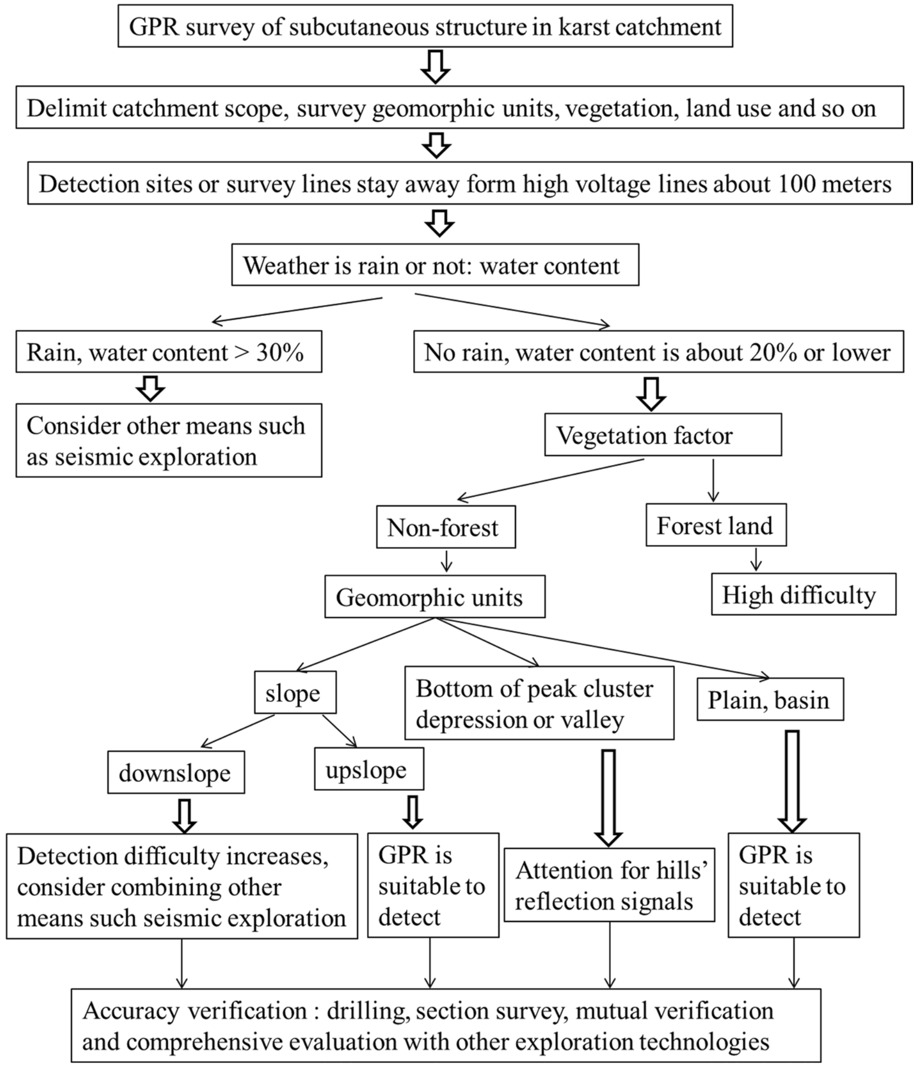

Fig. 17 Application potential paradigm of GPR to shallow surface structure in karst catchment

observations at different sites in the Houzhai river catchment. We combined with geomorphology, vegetation, moisture content, high voltage lines and other influencing factors, and evaluated the application potential of GPR in detecting surface soil and epikarst at the catchment scale. The degree of application potential evaluation answers the reliability of GPR data interpretation results acquired in different regions of the catchment. We developed initially the corresponding potential degree map of the Houzhai catchment. We've come up with one significant conclusion: the potential degree of GPR applied in the Houzhai catchment can be roughly divided into three different regions: high, moderate and low. The corresponding evaluation potential map and suggesting factors' index are expected to help investigators who are unfamiliar with GPR or the karst environment to have a macroscopic perspective. Simultaneously, the present study hopes to throw out a "brick" to attract more "jades" of further studies of professional GPR experts.

Supplementary Information The online version contains supplementary material available at https://doi.org/10.1007/s12665-023-11200-x.

Acknowledgements We thank two anonymous reviewers for the constructive and professional reviews and comments that improved this manuscript.

Author contributions QG wrote the original manuscript and did most work. YH improved the manuscript and discussed many contents. LC mapped some figures and participated filed work. DC gave some key ideas and discussions.

Funding The authors have not disclosed any funding.

Data availability The datasets in this study are available from the corresponding author upon reasonable request.

Declarations

Conflict of interest The authors declare no competing interests.

References

Alani AM, Lantini L (2020) Recent advances in tree root mapping and assessment using non-destructive testing methods: a focus on ground penetrating radar. Surv Geophys 41:605–646. https://doi.org/10.1007/s10712-019-09548-6

Al-fares W, Bakalowicz M, Guérin R, Dukhan M (2002) Analysis of the karst aquifer structure of the Lamalou area (Hérault, France) with ground penetrating radar. J Appl Geophys 51:97–106. https://doi.org/10.1016/S0926-9851(02)00215-X

Bahorich M, Farmer S (1995) 3-D seismic discontinuity for faults and stratigraphic features: The coherence cube. Lead Edge 14:1053–1058. https://doi.org/10.1190/1.1437077

Barna JM, Fryar AE, Cao L et al (2020) Variability in groundwater flow and chemistry in the Houzhai Karst Basin, Guizhou Province, China. Environ Eng Geosci 26:273–289. https://doi.org/10.2113/EEG-2306

Brandt M, Yue Y, Wigneron JP et al (2018) Satellite-observed major greening and biomass increase in South China karst during recent decade. Earth's Future 6:1017–1028. https://doi.org/10.1029/2018EF000890

Campbell JE (1990) Dielectric properties and influence of conductivity in soils at one to fifty megahertz. Soil Sci Soc Am J 54(2):332–341. https://doi.org/10.2136/sssaj1990.03615995005400020006x

Carbonel D, Rodríguez V, Gutiérrez F et al (2014) Evaluation of trenching, ground penetrating radar (GPR) and electrical resistivity tomography (ERT) for sinkhole characterization. Earth Surf Proc Land 39:214–227. https://doi.org/10.1002/esp.3440

Carcione JM, Seriani GS, Gei D (2003) Acoustic and electromagnetic properties of soils saturated with salt water and NAPL. J Appl Geophys 52:177–191. https://doi.org/10.1016/S0926-9851(03)00012-0

Čeru T, Šegina E, Knez M et al (2018) Detecting and characterizing unroofed caves by ground penetrating radar. Geomorphology 303:524–539. https://doi.org/10.1016/j.geomorph.2017.11.004

Chen H, Fu W, Wang K et al (2006) Dynamic change of soil water in peak-cluster depression areas of Karst Mountainous Region in Northwest Guangxi. Bull Soil Water Conserv 20:136–139. https://doi.org/10.13870/j.cnki.stbcxb.2006.04.033. (**in Chinese**)

Cheng J, Pan D, Li W et al (2010) Study on the detecting of hazard abandoned workings by ground penetrating radar on strong electromagenetic interference area. J China Coal Soc 35(2):227–231. https://doi.org/10.1322/j.cnki.jccs.2010.02.017. (**in Chinese**)

Cheng Q, Tao M, Chen X et al (2019) Evaluation of electrical resistivity tomography (ERT) for mapping the soil–rock interface in karstic environments. Environ Earth Sci 78:1–14. https://doi.org/10.1007/s12665-019-8440-8

Cheng Q, Wang S et al (2020) Sediment sources, soil loss rates and sediment yields in a Karst plateau catchment in Southwest China. Agr Ecosyst Environ 304:107114. https://doi.org/10.1016/j.agee.2020.107114

Coulouma G, Samyn K, Grandjean G et al (2012) Combining seismic and electric methods for predicting bedrock depth along a Mediterranean soil toposequence. Geoderma 170:39–47. https://doi.org/10.1016/j.geoderma.2011.11.015

Desper DB, Link CA, Nelson PN (2015) Accurate water-table depth estimation using seismic refraction in areas of rapidly varying subsurface conditions. Near Surf Geophys 13:455–465. https://doi.org/10.3997/1873-0604.2015039

Ding W, We Wu, Wang C, Wu Z (2014) Propagation characteristics of seismic waves in shallow soil with the unsaturated three-phase poroelastic model. Acta Phys Sin 63:224301. https://doi.org/10.7498/aps.63.224301. (**in Chinese**)

Doolittle JA, Collins ME (1998) A comparison of EM induction and GPR methods in areas of karst. Geoderma 85:83–102. https://doi.org/10.1016/S0016-7061(98)00012-3

Doolittle JA, Minzenmayer FE, Waltman SW, Benham EC (2003) Ground penetrating radar soil suitability maps. J Environ Eng Geophys 8:49–56. https://doi.org/10.4133/JEEG8.2.49

Doolittle JA, Minzenmayer FE, Waltman SW et al (2007) Ground-penetrating radar soil suitability map of the conterminous United States. Geoderma 141:416–421. https://doi.org/10.1016/j.geoderma.2007.05.015

Doolittle J, Dobos R, Peaslee S et al (2010) Revised ground-penetrating radar soil suitability maps. J Environ Eng Geophys 15:111–118. https://doi.org/10.2113/JEEG15.3.111

dos Reis JA, de Castro DL, de Jesus TES, Filho FPL (2014) Characterization of collapsed paleocave systems using GPR attributes. J Appl Geophys 103:43–56. https://doi.org/10.1016/j.jappgeo.2014.01.007

Gao Q, Wang S, Peng T et al (2020) Evaluating the structure characteristics of epikarst at a typical peak cluster depression in Guizhou plateau area using ground penetrating radar attributes. Geomorphology 364:107015. https://doi.org/10.1016/j.geomorph.2019.107015

Gao Q, Hussain Y, Yang T (2022) Analysis of georadar responses on environmentally significant karst landform. PREPRINT (Version 1) available at Research Square. https://doi.org/10.21203/rs.3.rs-2290108/v1

Gizzi FT, Leucci G (2018) Global research patterns on ground penetrating radar (GPR). Surv Geophys 39:1039–1068. https://doi.org/10.1007/s10712-018-9475-1

Guo S, Zhu J, Wang C et al (2021) Study on the joint application of electrical and seismic exploration in the investigation of fissure and Karst cave in Fuling area. CT Theory Appl 30:49–59. https://doi.org/10.15953/j.1004-4140.2021.30.01.05.(inChinese)

Han X, Liu J, Zhang J, Zhang Z (2016) Identifying soil structure along headwater hillslopes using ground penetrating radar based technique. J Mt Sci 13:405–415. https://doi.org/10.1007/s11629-014-3279-7

Hussain Y, Rogerio U, Welitom B et al (2020) The potential use of geophysical methods to identify cavities, sinkholes and pathways for water infiltration. Water 12:2289. https://doi.org/10.3390/w12082289

Hussain Y, Seivane H, Gao Q et al (2023) Seismic signatures and site characterization of an intermittent stream in dry and flood conditions: an implication for soil losses and landslide triggering. Environ Earth Sci 82:295. https://doi.org/10.1007/s12665-023-10960-w

Johnson RW, Glaccum R, Wojtasinski R (1979) Application of ground penetrating radar to soil survey. Soil Crop Sci Soc Florida Proc 39:68–72

Jol HM (2009) Ground penetrating radar: theory and applications. Elsevier Science, Amsterdam

Li S, Liu C, Li J et al (2010) Geochemistry of dissolved inorganic carbon and carbonate weathering in a small typical karstic catchment of Southwest China: isotopic and chemical constraints. Chem Geol 277:301–309. https://doi.org/10.1016/j.chemgeo.2010.08.013

Li L, Xia Y, Liu S et al (2015) Modified method for estimating organic carbon density in discontinuous Karst soil using ground-penetrating radar and geostatistics. J Mt Sci 12:1229–1240. https://doi.org/10.1007/s11629-015-3431-z

Pasquet S, Bodet L, Bergamo P et al (2016) Small-scale seismic monitoring of varying water levels in granular media. Vadose Zone J 15:1–14. https://doi.org/10.2136/vzj2015.11.0142

Schellentrager GW, Doolittle JA, Calhoun TE, Wettstein CA (1988) Using ground-penetrating radar to update soil survey information.

Soil Sci Soc Am J 52:746–752. https://doi.org/10.2136/sssaj1988.03615995005200030027x
Šumanovac F, Weisser M (2001) Evaluation of resistivity and seismic methods for hydrogeological mapping in karst terrains. J Appl Geophys 47:13–28. https://doi.org/10.1016/S0926-9851(01)00044-1
Tao M, Chen X, Cheng Q, Binley A (2022) Evaluating the joint use of GPR and ERT on mapping shallow subsurface features of karst critical zone in southwest China. Vadose Zone J. https://doi.org/10.1002/vzj2.20172
Tardío G, González-Ollauri A, Mickovski SB (2016) A non-invasive preferential root distribution analysis methodology from a slope stability approach. Ecol Eng 97:46–57. https://doi.org/10.1016/j.ecoleng.2016.08.005
Tong X, Brandt M, Yue Y et al (2018) Increased vegetation growth and carbon stock in China karst via ecological engineering. Nat Sustain 1:44–50. https://doi.org/10.1038/s41893-017-0004-x
Valois R, Camerlynck C, Dhemaied A et al (2011) Assessment of doline geometry using geophysics on the Quercy plateau karst (South France). Earth Surf Proc Land 36:1183–1192. https://doi.org/10.1002/esp.2144
Yan D, Zhang X, Wen A et al (2012) Assessment of sediment yield in a small karst catchment by using 137Cs tracer technique. Int J Sedim Res 27:547–554. https://doi.org/10.1016/S1001-6279(13)60012-8
Yang J, Zhang C (2014) Earth's critical zone: a holistic frame for geo-environment researches. Hydrgeology & Engineering Geology 41:98–104, 110. https://doi.org/10.16030/j.cnki.issn.1000-3665.2014.03.012. (**in Chinese**)
Yang J, Chen H, Nie Y, Wang K (2019) Dynamic variations in profile soil water on karst hillslopes in Southwest China. CATENA 172:655–663. https://doi.org/10.1016/j.catena.2018.09.032
Zajícová K, Chuman T (2019) Application of ground penetrating radar methods in soil studies: a review. Geoderma 343:116–129. https://doi.org/10.1016/j.geoderma.2019.02.024
Zhang Z, Chen X, Cheng Q et al (2011) Hydrogeology of epikarst in karst mountains—a case study of the Chenqi catchment. Earth Environ 39:19–25. https://doi.org/10.14050/j.cnki.1672-9250.2011.01.016. (**in Chinese**)
Zhang C, Qi X, Wang K et al (2017) The application of geospatial techniques in monitoring karst vegetation recovery in southwest China: a review. Prog Phys Geogr 41:450–477. https://doi.org/10.1177/0309133317714246
Zhang Z, Zhou Y, Wang S et al (2018) Change in SOC content in a small karst basin for the past 35 years and its influencing factors. Arch Agron Soil Sci 64:2019–2029. https://doi.org/10.1080/03650340.2018.1474520
Zhao W, Forte E, Pipan M et al (2013) Ground penetrating radar (GPR) attribute analysis for archaeological prospection. J Appl Geophys 97:107–117. https://doi.org/10.1016/j.jappgeo.2013.04.010
Zhou J, Tang Y, Yang P et al (2012) Inference of creep mechanism in underground soil loss of karst conduits I. Concept Model Nat Haz 62:1191–1215. https://doi.org/10.1007/s11069-012-0143-3

Publisher's Note Springer Nature remains neutral with regard to jurisdictional claims in published maps and institutional affiliations.